Determining Best Estimates and Uncertainties in Cloud Microphysical Parameters from ARM Field Data: Implications for **Models, Retrieval Schemes and Aerosol-Cloud-Radiation Interactions**

PI: Greg McFarquhar, University of Illinois, Dept. of Atmospheric Sciences, 105 S. Gregory Street, Urbana, IL 61801-3070 (217)265-5458 phone, (217)244-4393 fax, mcfarq@illinois.edu

Final Report December 2015

We proposed to analyze in-situ cloud data collected during ARM/ASR field campaigns to create databases of cloud microphysical properties and their uncertainties as needed for the development of improved cloud parameterizations for models and remote sensing retrievals, and for evaluation of model simulations and retrievals. In particular, we proposed to analyze data collected over the Southern Great Plains (SGP) during the Mid-latitude Continental Convective Clouds Experiment (MC3E), the Storm Peak Laboratory Cloud Property Validation Experiment (STORMVEX), the Small Particles in Cirrus (SPARTICUS) Experiment and the Routine AAF Clouds with Low Optical Water Depths (CLOWD) Optical Radiative Observations (RACORO) field campaign, over the North Slope of Alaska during the Indirect and Semi-Direct Aerosol Campaign (ISDAC) and the Mixed-Phase Arctic Cloud Experiment (M-PACE), and over the Tropical Western Pacific (TWP) during The Tropical Warm Pool International Cloud Experiment (TWP-ICE) to meet the following 3 objectives:

a. derive statistical databases of single ice particle properties (aspect ratio AR, dominant habit, mass, projected area) and distributions of ice crystals (size distributions SDs, mass-dimension *m-D*, area-dimension *A-D* relations, mass-weighted fall speeds, single-scattering properties, total concentrations *N*, ice mass contents *IWC*), complete with uncertainty estimates;

b. assess processes by which aerosols modulate cloud properties in arctic stratus and mid-latitude cumuli, and quantify aerosol's influence in context of varying meteorological and surface conditions;

c. determine how ice cloud microphysical, single-scattering and fall-out properties and contributions of small ice crystals to such properties vary according to location, environment, surface, meteorological and aerosol conditions, and develop parameterizations of such effects.

Below we describe the accomplishments that we made on all 3 research objectives.

a. Statistical databases of single particle properties:

A key measurement need for models and retrievals is information about ice crystal habit because microphysical and radiative properties of ice clouds depend heavily on crystal shapes. Thus, under prior ASR funding we had developed a quasi-automatic habit classification (Um and McFarquhar 2009) that sorts ice crystals imaged by a Cloud Particle Imager (CPI) into 11 categories (Figure 1). Under the funding provided by the current grant, we completed the categorizations for several flights during TWP-ICE and SPARTICUS, concentrating on flights noted as of interest by Ann Fridlind and other ASR funded investigators for their modeling studies (see Table 1 for complete list of flights analyzed). To assess the accuracy of our classification scheme, we compared results from our manual classification scheme and from an

automated classification scheme that we developed with those from other habit classification schemes, namely those used at the University of Helsinki (Lindqvist et al. 2012, a scheme that we collaborated in the development of) and at Blaise Pascal University. This work was started in the summer of 2012 during the visit of the PI to Clermont-Ferrand in France, and has tested agreement between different classification schemes as a function of a location (mid-latitudes, Arctic, or Tropics), cloud type, formation mechanism, and meteorology. Although we did not complete the journal article describing the results of this comparison, we anticipate writing a publication for the *Journal of Atmospheric and Oceanic Technology* describing this work in the near future (Um et al. 2016a). Components of this work have also been presented at the ASR Science Team Meetings.

We also determined how aspect ratios of ice crystals vary with environmental conditions. Previous studies showed that the aspect ratio, the ratio between crystal width W and length L, is a key parameter because it is input to calculations of the single-scattering properties of ice crystals and determines the microphysical properties of ice crystals, such as the cross-sectional area and fall velocity which are incorporated into parameterizations used in numerical models and satellite retrievals. Past studies have quantified the L-W relationship or aspect ratio (AR) of natural ice crystals based on laboratory measurements and in-situ data. However, most such work was based on a very limited number of measured crystals observed within limited temperature and humidity ranges in a single geographic regime. We have considerably extended these past efforts by using a much larger number of ice crystals imaged in a variety of conditions and locations to determine what controls of L-W relationships and ARs of individual crystals.

In particular, we measured the dimensions of hexagonal prisms (i.e., columns and plates) and individual branches of bullet rosettes using high-resolution ice crystal images recorded by a CPI during TWP-ICE, ISDAC and SPARTICUS. New software, henceforth the "Ice Crystal Ruler (IC-Ruler)", which measures the dimensions of ice crystal images, was developed at the University of Illinois as part of this funding cycle by M.S. student Sunkyu Kim. Using this software, the maximum dimension, length, and width of many ice crystal images was determined. Figure 2 shows selected CPI images of bullet rosettes, columns, and plates, together with an illustration of how their dimensions were measured using the IC-Ruler. Since crystal images are two-dimensional and the crystals themselves are three dimensional, the measured dimensions of ice crystals are projections of actual dimensions. Therefore, an iterative approach was applied to quantify the relationship between actual length, width, and aspect ratio of the three-dimensional ice crystals based on the corresponding measurements of their projections in two-dimensional space. This allowed the derivation of a power low describing the true relationship between the length and width of ice crystals.

All CPI data acquired during TWP-ICE and ISDAC and approximately 50% of the SPARTICUS data were analyzed to derive L, W, and AR. The same procedure can be applied to other field campaign data. Results have been shown during several invited seminars, during the DOE ASR Meetings, the 2013 AGU Fall Meeting, the American Meteorological Society *14th Conference on Cloud Physics* and the American Meteorological Society *14th Conference on Atmospheric Radiation*. Two research papers were written, one published in *Atmospheric Chemistry and Physics* (Um et al. 2015) and the other which has been submitted to *Atmospheric Chemistry and Physics* (Fridlind et al. 2015) describing the technique itself, and application of it to improve and evaluate model parameterizations, respectively.

It is important to know the shape of small particles in mixed-phase clouds because this gives information about the phase of these particles, which controls not only the radiative impact of the cloud but also the microphysical processes occurring in cloud that controls its lifetime. In a paper published in the *Journal of Applied Meteorology and Climatology* (McFarquhar et al. 2013), we analyzed the shapes of cloud particles with maximum dimensions between 35 and 60 μm in mixed-phase clouds using images acquired by the CPI during M-PACE and ISDAC. We were able to identify particle sizes and probe focusing conditions under which reliable shape information about such small particles could be obtained, and showed that the average area ratio of these small cloud particles was correlated with the ratio of liquid water content to total water content, with the correlations stronger when larger liquid cloud droplets were present. The most important finding of our study was that the assumption that all small particles in mixed-phase clouds are supercooled water droplets, does not hold true.

Another important issue that we investigated while conducting our work on determining how SDs and associated bulk cloud parameters vary with environmental conditions was to determine the degree to which the shattering of large ice crystals on probe tips artificially amplifies the concentrations of small ice crystals. Although shatter reducing tips and correction algorithms to remove shattering artifacts exist and are now used in most ARM experiments, there is considerable uncertainty in their effectiveness. Significant progress has been made in determining the degree to which shattering on newly designed probe tips contaminates measured SDs and bulk parameters, and in determining the degree to which data previously collected by conventional probes is contaminated by shattering.

In a manuscript published in the *Journal of Atmospheric and Oceanic* technology (Jackson et al. 2014) we compared number distribution functions *N(D)* from 2D Cloud Probes (2DCs) with standard and modified tips and processed with and without state-of-art shattered artifact removal algorithms using data acquired during ISDAC and the Instrumentation Development and Education in Airborne Science-2011 (IDEAS-2011). We estimated how the contributions of shattered artifacts to *N(D)* varied as a function of particle size, shape, concentration, degree of riming, temperature, true air speed, and aircraft attitude and attack angles. Figure 3 shows how the ratio of the number concentration from the 2DC with standard tips divided by the 2DC with modified tips N_s/N_m for differing size ranges varied as a function of median mass diameter D_{mm}. The subscript (*na*) indicates that shattered artifact removal algorithms were not applied while the subscript (*a*) indicates that they were. It is seen that $N_{s\text{-}na}/N_{m\text{-}na}$ and $N_{s\text{-}a}/N_{m\text{-}a}$ increase with D_{mm} and are greater than 2 for $D_{mm} > 1$ mm. The increase of $N_{s\text{-}na}/N_{m\text{-}na}$ with D_{mm} is consistent with previous studies that showed the likelihood of particle shattering was related to particle size due to the higher energies of the larger particles. N_s/N_m was also found to be higher when graupel or riming was present. A series of Monte Carlo simulations with varying ice crystal concentrations, numbers of shattered particles, length of train of shattered fragments, and probabilities of shattered particles entering the sample volume was conducted and used to interpret the measured distribution of particle interarrival times by the 2DCs and showed that differences in frequency distributions of interarrival times can be caused by differences in true air speeds, natural particle concentrations, probe sample volumes and geometries, as well as differences in ice particle habit, size, density, impact velocity, temperature, or angle of attack. This work was presented at the *16th International Conference on*

Clouds and Precipitation in Leipzig, Germany, the *NCAR Lower Atmospheric Facilities Observing Workshop*, the *4th ASR Science Team meeting* and the *American Geophysical Union Fall Meeting*.

A second manuscript also published in the *Journal of Atmospheric and Oceanic Technology* (Jackson and McFarquhar 2014) assessed the impact of large crystal shattering on probe tips on bulk parameters that are derived from the size distribution data. In particular, the impact of shattering on the bulk extinction β, ice water content *IWC*, median diameter D_m, median mass diameter D_{mm}, mass weighted terminal velocity v_m, effective radius r_e, asymmetry parameter g, and single scatter albedo ω derived from 2DC data is derived by comparing values derived from probes with standard and modified tips and processed with and without shattered artifact removal algorithms. Data from ISDAC and IDEAS-2011 were again used. Since numerous model parameterization and remote sensing schemes as well libraries of ice cloud microphysical properties use bulk properties derived from 2DC data, the impact of this study is immense. Figure 4 plots β derived from probes without the modified tips and derived without the shatter removing algorithms as a function of β_m^a, where the superscript (*na*) again indicates that shattered artifact removal algorithms were not applied while superscript (*a*) denotes when they are used, and the subscript *s* denotes when standard tips were used and *m* when modified tips were used. Figure 4 shows the modified tips reduced β by 15% and the algorithms by 25%. Using either modified tips and/or algorithms changed *IWC*, D_{mm}, r_e, g, and ω by at most 25%, which is less than the factor of 7 reductions seen for number concentration or factor of 5 increases in median particle diameter. Changes in ω and g of less than 0.01 are less than the certainty at which they need to be known from a climate modeling perspective. This shows that bulk ice microphysical and optical properties derived from higher order moments of the 2DC size distribution are biased by shattering to a much smaller degree than properties derived from lower order moments such as number concentrations. Therefore the use of bulk microphysical properties derived from higher order moments of ice SDs from historical 2DC datasets in model parameterizations and remote sensing schemes is likely still appropriate. However, parameterizations and schemes based on lower order moments such as median diameter and number concentration may contain significant biases. This work was presented at the *5th ASR Science Team Meeting* and will be presented at the *14th American Meteorological Society Conference on Cloud Physics*.

In addition to the impact of shattering on derived SDs and bulk cloud properties, other sources of uncertainty arise from the algorithms that convert raw particle probe data into derived products. One of these uncertainties that we have been exploring is the definition of particle maximum dimension (D_{max}) that is used to derive the number distribution function, $N(D_{max})$, that characterizes the SDs. Many algorithms that analyze two-dimensional particle images acquired by in-situ imaging probes use different definitions of D_{max} for deriving SDs. Common definitions include maximum length in the horizontal or photodiode array direction (D_P), maximum length in vertical or time direction (D_T), and their combinations, such as $\frac{1}{2}(D_P+D_T)$ and $\sqrt{D_P^2 + D_T^2}$. The diameter of the minimum circle enclosing the particle has also been used. Figure 5 shows that the $N(D_{max})$ can vary by up to an order of magnitude in some size ranges when using different definitions of D_{max}. Substantial differences in the fit parameters of gamma distributions (N_0, μ and λ) used to characterize $N(D_{max})$ are also seen. The use of different

definitions of D_{max} also affects the calculation of bulk cloud and optical properties. For example, *IWC,* β, and r_e calculated by mass- and area-dimensional relations can vary by 2-3 times. Further, the mass-weighted terminal velocity can differ by 60%, and precipitation rate by one order of magnitude, leading to differences in microphysical process rates used in numerical models. These differences occur because fundamental relationships used to derive the bulk properties, such as relations for particle velocity and mass with particle dimension, are identically applied regardless of the D_{max} definition used. The uncertainties in derived SDs using different definitions can propagate to these calculated bulk properties through the same model. These differences show the need to use consistent definitions of D_{max} for defining $N(D_{max})$ and the functional dependence of particle microphysical properties on D_{max}. A paper describing this work has been accepted with minor revisions for the *Journal of Atmospheric and Oceanic Technology* (Wu and McFarquhar 2016a) and was presented at the *5th ASR Science Team Meeting*, and at the *14th American Meteorological Society's Conference on Cloud Physics*.

b. Aerosol modulation of cloud properties

Our first accomplishment in this topic area was the completion of a paper for the *Journal of the Atmospheric Sciences* (Jackson et al. 2012) that described how ice microphysical properties in arctic mixed-phase stratus depended on aerosol concentrations. Using data collected during ISDAC, we showed that the liquid droplet concentration was well correlated with the aerosol number concentration below cloud and that the ice crystal number concentration was well correlated with the aerosol concentration above cloud. The profiles of microphysical quantities were consistent with the mixing of ice nuclei from cloud top consistent with a glaciation indirect effect. The lower ice crystal concentrations and liquid effective radii for the ISDAC cases compared to data collected in clearer single-layer stratocumulus during M-PACE was consistent with the thermodynamic indirect effect. However, due to the large scatter in our results, we noted that more data were required in a wider variety of surface conditions and meteorological forcing to identify the dominant aerosol forcing mechanisms operating in mixed-phase arctic clouds.

We also used our ISDAC analysis in a collaborative study (Zamora et al. 2016) to explore cloud microphysics in liquid-phase clouds influenced by biomass burning using data from several arctic field projects. It was found that median cloud droplet radii in smoky clouds were ~50% smaller than in background clouds. Based on the relationship between cloud droplet number (N_{liq}) and various biomass burning tracers (BB_t) across the multi-campaign dataset, the magnitude of subarctic and Arctic smoke aerosol-cloud interactions (ACI, where ACI = (1/3)* d $\ln(N_{liq})$/d $\ln(BB_t)$) was calculated to be ~0.12 out of a maximum possible value of 0.33 that would be obtained if all aerosols were to nucleate cloud droplets. This analysis showed that the smoke-driven cloud albedo effect may decrease local summertime shortwave radiative flux by 2-4 W m^{-2} or more under some low and homogeneous cloud cover conditions in the subarctic, although the changes should be smaller in high surface albedo regions of the Arctic. This work was presented at the 2014 American Geophysical Union meeting and the 2015 Canadian Meteorological and Oceanographic Society meeting.

In addition, graduate student Hee-Jung Yang continued her analysis of data collected in fair weather cumuli over the SGP site during RACORO. During the 2009 field campaign, a total

of 260 hours of in-situ airborne cloud and aerosol measurements were made over a period of 6 months, with 85 hours of data collected on days when shallow cumuli were present in varying meteorological regimes. Aerosol-cloud interactions in shallow cumuli over Southern Great Plain (SGP) region were investigated by examining how cloud properties vary with aerosol concentration and meteorological conditions. Her earlier analysis reached the conclusion that variations in vertical velocity were more important than variations in aerosol concentrations in defining the cloud properties. Yang and McFarquhar (2012) also examined the impact of variations in aerosol forcing on the entrainment and detrainment processes occurring in these fair weather cumuli, showing that near cloud top the mixing was more homogeneous (mixing first and evaporation later) whereas near cloud base there was extreme inhomogeneous mixing (evaporation first followed by mixing). However, it has been difficult to isolate aerosol effects on clouds in these prior studies because of the complicated microphysical and dynamical feedbacks that occur. To avoid complications and ambiguity, we are now investigating the aerosol effects in context of the synoptic meteorology of the Great Plain region. The RACORO fair weather cumuli days have been grouped into 5 different categories according to the airmass source regions and meteorological characteristics, and the relationship between aerosol and cloud properties is now being separately investigated for each category. These results were presented at the *American Meteorological Society 14th Conference on Cloud Physics Conference*, the 2015 Annual Meeting of the American Meteorological Society and at Panorama Actual de las Ciencias Atmosféricas 2015, Universidad Nacional Avtonoma de Mexico (McFarquhar 2015). The concept of collecting routine data over a several month long field campaign was also presented at the First Conference of the International Society for Atmospheric Research using Remotely Piloted Aircraft (ISARRA). Further, we are expecting that a paper will be submitted to the *Journal of the Atmospheric Sciences* describing the results of these studies (Yang and McFarquhar 2016).

We also used the RACORO data in collaboration with K.S. Lim in a study involving evaluation of a new cloud-droplet number concentration (NDROP) value added product (VAP) for single-layer warm clouds (Lim et al. 2016) based on measurements of cloud optical depth from the multi-filter rotating shadow-band radiometer (MFRSR) and liquid water path from the microwave radiometer (MWR). The RACORO data showed that the VAP reproduces the primary mode of the in situ measured probability density function (PDF), but produces a too wide distribution, primarily caused by frequent high cloud-droplet number concentration. Consideration of entrainment effects rather than assuming an adiabatic cloud improves the values of the NDROP retrieval by reducing the magnitude of cloud-droplet number concentration. Comparisons with the RACORO data suggested that the vertical distribution of cloud-droplet number concentration and effective radius was feasible with an improvement of the parameter representing the mixing effects between environment and clouds and with a better understanding of the effect of mixing degree on cloud properties.

In another collaborative study (Endo et al. 2015), we provided our analysis of RACORO microphysical properties to evaluate simulations of continental boundary layer cumulus clouds from two large-eddy simulation (LES) models. It was found that the LES simulations capture the in-situ observed and remote sensing detected transitions of the evolving cumulus-topped boundary layers during the three daytime periods, and generally reproduced variations of droplet number concentration with LWC, corresponding to the gradient between the cloud centers and

cloud edges at given heights. The observed LWC values fell within the range of simulated values; the observed droplet number concentrations were commonly higher than simulated, but differences remain on par with potential estimation errors in the aircraft measurements. This work was also presented at the Fall Meeting of the *American Geophysical Union*.

The effects of aerosols on evaporation, freezing and precipitation in a multiple cloud system in the Tropics were also investigated using a modeling simulation. Two-day simulations were performed for a mesoscale cloud ensemble (MCE) observed during the TWP-ICE. Previous studies on single-cloud systems had shown that aerosol-induced increases in freezing and associated increases in parcel buoyancy were main mechanisms controlling aerosol-precipitation interactions in convective clouds. However, in the multiple cloud system, aerosol effects on evaporation as well as aerosol effects on freezing affected the aerosol-precipitation interactions. While aerosol-induced increases in freezing created intermittent heavy precipitation, aerosol-induced increases in evaporation enhanced the light precipitation. This increase in light precipitation made it possible for the cumulative precipitation to increase with increasing aerosol concentration, even though the increase was small. One research paper has been accepted with minor revision in the *Earth and Planetary Science Letters* (Lee et al. 2014) describing this effort.

c. Determining dependence of ice cloud properties on environmental conditions

Gamma distributions are frequently used to represent particle size distributions (SDs) in mesoscale and cloud resolving models that predict 1, 2 or 3 bulk moments of hydrometeor species. They are characterized by intercept (N_0), slope (λ) and shape (μ) parameters determined by fits to SDs measured in-situ. Before starting to develop fits to ice crystal SDs measured during ARM field campaigns, we examined the strengths and weaknesses of different techniques used to determine fit parameters and developed a new fitting technique called the Incomplete Gamma Fit (IGF) technique. Using data acquired in arctic cirrus during ISDAC we have shown that N_0, λ and μ are not independent parameters, but rather exhibit mutual dependence. They are also sensitive to the tolerance permitted by fitting algorithms, meaning a 3-dimensional volume in N_0-λ–μ phase space is required to represent a single SD. The tolerance allowed in the fit, which controls the size of this volume, is determined by the statistical uncertainty in the measured SD. Parameters within this volume of equally realizable solutions can vary substantially with N_0, in particular, spanning several orders of magnitude depending on the tolerance chosen. The dependence of the fit parameters on choice of fitting technique is not as large. A method to characterize a family of SDs as an ellipsoid in $N_0/\lambda/\mu$ phase space has also been developed, with the associated scatter in $N_0/\lambda/\mu$ for such families comparable to scatter in N_0, λ, and μ observed in prior field campaigns conducted in different conditions. Ramifications for the development of cloud parameterization schemes and associated calculations of microphysical process rates are also being considered. The results of this study have been published in the *Journal of the Atmospheric Sciences* (McFarquhar et al. 2015) and have been presented at the *American Geophysical Union Fall Meeting*, the *5th ASR Science Team Meeting* and at the *American Meteorological Society's 14th Conference on Cloud Physics*. We are currently developing methodologies for determining how the $N_0/\lambda/\mu$ surfaces vary with environmental parameters. In future years, we will apply these techniques to SDs measured in other field projects and investigate how the parameters vary with environmental conditions.

Using our understanding of the uncertainties in measured SDs and our techniques for fitting SDs to gamma functions, we used data from a wide variety of ARM/ASR field campaigns to examine how the microphysical properties of ice clouds vary with environmental conditions (e.g., temperature, relative humidity, depth in cloud), cloud formation mechanism (synoptic scale lifting, thunderstorm anvils, orographic lifting) and geographic location (Tropics, mid-latitudes, Arctic). We published a manuscript in the *Journal of Geophysical Research* (Jackson et al. 2015) that shows how the ice microphysical properties observed during SPARTICUS vary as a function of temperature, formation mechanism, and vertical velocity. Figure 6 shows an example of the approach we used where we show that β increases with temperature for synoptic cirrus, but any trend for the variation of β with temperature for anvil cirrus was not statistically significant. This shows that ice crystals are able to grow more effectively at warmer temperatures in synoptic cirrus due to processes like vapor diffusion and aggregation. But, for anvil cases, β is constant with temperature and is larger (~2 km^{-1}) at a temperature of -50˚C compared to synoptic cirrus (~0.5 km^{-1}). This occurs because updrafts in thunderstorms transport ice from warmer to colder temperatures. In addition, in Jackson et al. (2015) we modified our existing approach to represent a size distribution (SD) as a single gamma function using an ellipsoid of equally realizable solutions in (N_0, λ, μ) phase space to automatically identify multiple modes in SDs and characterize each mode by such an ellipsoid. The modified approach was applied to ice crystals with maximum dimension D > 15 μm collected by the 2D stereo and 2D precipitation probes on the Stratton Park Engineering Company (SPEC) Learjet. The dependencies of N_0, μ, λ from each mode, total number concentration, bulk extinction, ice water content, and mass median maximum dimension D_{mm} as a function of temperature T and cirrus type were analyzed. The changes in the observed codependencies between N_0, μ, and λ with environmental conditions indicated that particles were larger at higher temperatures during SPARTICUS. At most two modes were observed in any SD, and the average boundary between them was at 115 μm, similar to past studies. The bimodality of SDs increased with T. This and differences in N_0, μ, and λ between modes suggest that particles with smaller D nucleated more recently than particles with larger D, which grew via vapor deposition and aggregation. Because smaller crystals whose concentrations are uncertain make marginal contributions to higher order moments, the use of higher moments for evaluating model fields is suggested. This work was presented at the *5th ASR Science Team Meeting* and at the *American Meteorological Society's 14th Conference on Cloud Physics*.

Similar analysis has been conducted with data collected during MC3E by graduate student Wei Wu and preliminary results were presented at the ASR Fall Working Group Meetings. We used the in-situ probe data collected on 18 May, 20 May, 23 May and 24 May 2011 to characterize how the statistical distributions of *IWC* and r_e varied with temperature, supersaturation, vertical velocity and turbulence. An example of the analysis is presented in Figure 7, where the frequency distributions of *IWC* are seen as a function of temperature. In general, we saw that *IWC* decreased with temperature for temperatures less than -25˚C, with less dependence on temperature for greater than -25˚C. We also found that *IWC* decreased with saturation ratio when the air was sub-saturated, but there was little increase in *IWC* with the amount of supersaturation. We also found that IWC increased with vertical velocity, but had little dependence with turbulence. There was a big increase of r_e for temperatures larger than -25˚C, and a bifurcation of r_e for supersaturated conditions. The r_e increased with vertical velocity, and had little dependence on the amount of turbulence. Ongoing work is characterizing

the dependence of other bulk variables on these same parameters, with the ultimate goal of comparing against trends in data obtained during other field projects as the function of the same variables. We anticipate writing a publication for *Atmospheric Chemistry and Physics* in the next year summarizing these results (Wu and McFarquhar 2016b).

We also proposed to determine the dependence of mean single-scattering properties of distributions of ice crystals on environmental conditions. But, to calculate mean scattering properties, we first needed libraries of single-scattering properties for different idealized models of ice crystals. To determine these libraries, we use numerical codes to compute scattering properties for specific orientations, and then average over several different orientation angles. Hence, efficient averaging schemes are required. We examined the optimal orientation averaging scheme (regular lattice grid scheme or quasi Monte Carlo (QMC) method), the minimum number of orientations, and the corresponding computing time required to calculate the average single-scattering properties (i.e., g, ω_0, Q_{ext}, Q_{sca}, Q_{abs}, and scattering phase function at scattering angles of 90° (P_{11} (90°)), and 180° (P_{11} (90°))) within a predefined accuracy level (i.e., 1.0%) for 4 realistically shaped nonspherical atmospheric ice crystal models (Gaussian random sphere, droxtal, budding Bucky ball, and column) with D=10 μm using the Amsterdam discrete dipole approximation (ADDA) at λ=0.55, 3.78, and 11.0 μm (Um and McFarquhar 2013). The QMC required fewer orientations and less computing time than the lattice grid. The minimum number of orientations and the corresponding computing time decreased with an increase of wavelength, whereas they increased with the surface-area ratio that defines particle non-sphericity.

The optimal orientation averaging scheme (regular lattice grid scheme or quasi Monte Carlo (QMC) method), the minimum number of orientations, and the corresponding computing time required to calculate the average single-scattering properties (i.e., asymmetry parameter (g), single-scattering albedo (ω_0), extinction efficiency (Q_{ext}), scattering efficiency (Q_{sca}), absorption efficiency (Q_{abs}), and scattering phase function at scattering angles of 90° (P_{11} (90°)), and 180° (P_{11} (90°))) within a predefined accuracy level (i.e., 1.0%) were determined for four different realistically shaped nonspherical atmospheric ice crystal models (Gaussian random sphere, droxtal, budding Bucky ball, and column) with maximum dimension D=10 μm using the Amsterdam discrete dipole approximation (ADDA) at λ=0.55, 3.78, and 11.0 μm. The QMC required fewer orientations and less computing time than the lattice grid. For example, the use of QMC saved 55.4 (60.1, 46.3), 3,065 (117, 110), 3,933 (65.8, 104), and 381 (22.8, 16.0) hours of computing time for calculating the single-scattering properties (g, ω_o, Q_{ext}, Q_{sca}, Q_{abs}, P_{11} (90°), and P_{11} (180°)) within 1.0% accuracy for 3B, droxtal, Gaussian random sphere, and column, respectively, at λ=0.55 (3.78, 11.0) μm (Figure 8). The calculations of P_{11} (90°) and P_{11} (90°) required more orientations than the calculations of integrated scattering properties (i.e., g, ω_0, Q_{ext}, Q_{sca}, and Q_{abs}) regardless of the orientation average scheme. The fewest orientations were required for calculating g and ω_0. The minimum number of orientations and the corresponding computing time for single-scattering calculations decreased with an increase of wavelength, whereas they increased with the surface-area ratio that defines particle nonsphericity. These results were published in the *Journal of Quantitative Spectroscopy and Radiative Transfer* (Um and McFarquhar 2013).

Another proposal objective was to quantify how the contributions of small ice crystals smaller than 50 μm to cloud mass and radiative properties varied according to meteorology and

other environmental conditions. Small ice crystals are important because they can contribute, for example, more than 50% to the total projected area and hence to radiative properties of Arctic stratus. To calculate single-scattering properties of small ice crystals, idealized models representing shapes of small ice crystals are required. Current state-of-art cloud probe (i.e., CPI) possess large uncertainties in determining the shapes of these ice crystals due to limited resolution and contaminations due to diffraction at the wavelength at which a CPI works. Thus, we worked to compute the scattering properties of several idealized models commonly used to represent the shapes of small ice crystals (Gaussian random sphere, droxtal, budding Bucky ball, and column). Conventional ray-tracing codes used to calculate the scattering properties of large ice crystals cannot be applied to small ice crystals. Therefore, the discrete-dipole-approximation (DDA), also known as the coupled dipole approximation, was used to calculate the single-scattering properties of irregularly shaped particles. Using resources from the Extreme Science and Engineering Discovery Environment's (XSEDE) supercomputer Kraken, the NSF Petascale Computing Resource Allocation (PRAC) program's Blue Waters, and the Linux cluster within the Department of Atmospheric Sciences at the University of Illinois, the single-scattering properties of small ice crystals were calculated for crystals with dimensions less than 20, 50 and 50 μm at λ=0.55, 3.78, and 11.0 μm, respectively. An example result is shown in Figure 9. We are working on the remaining calculations using the clusters at University of Illinois and time that has recently been provided by XSEDE and NESRC. In addition to DDA, we have used a new *T*-matrix code called Tsym to calculate the single-scattering properties of a Gaussian random sphere and a column. This code is designed to compute single scattering properties of non-axisymmetric particles with finite symmetries (e.g., pentagonal or hexagonal column), which is distinct feature compared with a conventional *T*-matrix code. A comparison between the results from DDA and Tsym will be submitted to the *Journal of Quantitative Spectroscopy and Radiative Transfer* (Um and McFarquhar 2016b).

We have also performed work that examines atmospheric halo formation by hexagonal ice crystals because the results of such a study are needed to determine the range of applicability of the conventional geometric optic method for calculations of the scattering properties of small ice crystals. Hexagonal crystals (i.e., columns and plates) represent the building blocks of many common ice crystal habits. Previous studies have shown that atmospheric halos begin to form when the size parameter (ratio between size of particle and wavelength of incident light) of ice crystals increases to between 80 and 100, with the exact size parameter depending on the assumed geometry of the crystal, the method used to solve the radiative transfer equations, and the wavelength of incident light. The threshold size at which atmospheric halos emerge determines the applicability of the conventional geometric optic method on the calculations of scattering properties of small particles. The halo display is an intrinsic optical feature in the geometric optic regime, which is not shown in the resonant regime. In a study published in *Journal of Quantitative Spectroscopy and Radiative Transfer* (Um and McFarquhar 2015) we thus investigated how variations in the sizes and aspect ratios (*AR*, *L* and *W*) of ice crystals affect the size parameter at which haloes first emerge. High-resolution images of ice crystals obtained from aircraft probes during ARM/ASR projects were used to define the range in *AR* that different sized ice crystals have. Then, the single-scattering properties of hexagonal crystals with maximum dimensions up to 48 μm and *AR*s of 0.10, 0.25, 0.5, 1.0, 2.0, and 4.0 at a wavelength of 0.55 μm were calculated using DDA. From these accurate and large simulations, the threshold size at which 22° and 46° halos form was determined. Figure 10 shows the scattering phase

function P_{11} of six different *ARs* of hexagonal ice crystals with D=16 μm at λ=0.55 μm. Hexagonal crystals with *AR*=0.25 (Fig. 10b), 0.50 (Fig. 10c), 1.0 (Fig. 10d) show distinct 22° halo, whereas only hexagonal crystals with *AR*=0.50 and 1.0 produce the 46° halo. Both 22° and 46° halos are not shown for prolate hexagonal crystals (i.e., columns with $L > W$) as shown in Figs. 10e and 10f. Thus, the *AR* of crystals plays an important role in the formation of atmospheric haloes. The effects of size and *AR* of hexagonal crystals on the halo formation are further quantified defining the halo ratio (*HR*), where $HR=P_{11}(\theta_1)/P_{11}(\theta_2)$. Here, θ_1 and θ_2 are 22° and 18.5° for the 22° halo, whereas they are 46.5° and 43° for the 46° halo. The *HR* values larger than 1.0 (dotted black lines in Figure 11) indicate the presence of halo. Figure 11 shows that hexagonal crystals with small sizes cannot produce halo features even though they should be large enough to generate halos, in particular for the 46° halo. Further, both prolate (long columns) and oblate (thin plate) hexagonal crystals have difficulty to generate halos compared with compact crystals (e.g., *AR*=1.0). These results were shown during the 2014 Second Annual NCSA Blue Waters Symposium, the American Meteorological Society *14th Conference on Atmospheric Radiation,* the 2015 Third Annual NCSA Blue Waters Symposium for Petascale Science and beyond, and the 2015 XSEDE Science Conference.

Other Activities:

Our group participated in the following activities of relevance to ASR funded research:

1) PI was co-leader of the ASR Focus group on Ice Cloud Processes and Properties (IcePro). The PI was active in the development of the white paper describing this effort in the past year, and many of the deliverables in this report were completed by the PI's group in collaboration with other groups.
2) PI is serving on doctoral committee of Jingyu Wang at University of North Dakota. Jingyu is analyzing in-situ microphysical data collected during MC3E.
3) PI organized sessions on ice clouds at the Davos Atmosphere and Cryosphere Assembly (DACA-13) meeting in Davos, Switzerland
4) PI participated in the Polar atmospheric measurements workshop related to research using small unmanned aerial systems (UAS) in Washington, DC in July 2013.
5) PI participated in the North Slope Supersite Workshop in Washington DC in September 2014
6) PI organized a session on Clouds, aerosols and their influence on climate over the Southern and Antarctic Oceans as part of the 2015 IAMAS Symposium in Prague, Czech Republic
7) PI co-organized workshop on "Clouds, aerosols, precipitation, radiation and air-sea interface of the Southern Ocean: Establishing directions for future research" in Seattle, Washington in May 2014
8) The PI provided guidance to many groups who are using the Value Added Products that have been generated by his group for the RACORO, ISDAC and M-PACE field experiments. Some of these activities have resulted in co-authored papers (e.g., Verlinde et al. 2013; Hiranuma et al. 2013; Maahn et al. 2015) whereas others have resulted in papers that give a better use of the products without our participation as co-authors (e.g., papers by Chunsong Lu of BNL and Caroline Jouan of UQAM), and still other collaborations/data usages are ongoing (Ann Fridlind of NASA GISS, Bastiaan van Diedenhoven of Columbia University, Subashree Mishra of University of Oklahoma,

Wei-Kuo Tao of NASA GSFC, Rachel Atlas of the University of Chicago, Paivi Haapanala of the University of Helsinki, Vaughan Phillips of Leeds University, Laura Riihmaki of PNNL, Michael Earle of Environment Canada).

Publications and Deliverable Products, Conference Proceedings, and Seminars in Lifetime of Grant

Refereed publications published, submitted or to be submitted in near future are listed, together with conference presentations and presented seminars. Many of these papers and presentations are referenced in the above description of accomplishments, so this section also serves as a reference list.

Refereed Publications:

Baumgardner, D., L. Avallone, A. Bansemer, S. Borrmann, P. Brown, U. Bundke, D. Cziczo, P. Field, A. Heymsfield, A. Korolev, M. Kramer, G. McFarquhar, O. Mohler, S. Lance, P. Lawson, D. Rogers, O. Stetzer, J. Stith, C. Twohy, and M. Wendisch, 2012: In situ, airborne instrumentation: Addressing and solving measurement problems in ice clouds. Bull. Amer. Meteor. Soc., **93**, ES29-ES34.

Endo, S., A.M. Fridlind, W. Lin, A.M. Vogelmann, T. Toto, A.S. Ackerman, G.M. McFarquhar, R.C. Jackson, and Y. Liu, 2015: RACORO continental boundary layer cloud investigations. 2. Large eddy simulations of cumulus clouds and evaluation with in situ and ground-based observations. *J. Geophys. Res*., **120,** 5993-6014.

Fridlind, A.M., R. Atlas, B. van Diedenhoven, J. Um, G.M. McFarquhar, A.S. Ackerman, E.J. Moyer, and R.P. Lawson, 2015: Derivation of physical and optical properties of midlatitude cirrus ice crystals for a size-resolved microphysics model. *Atmos. Chem. Phys. Disc.*, Under review.

Hiranuma, N., S.D. Brooks, R.C. Moffet, A. Glen, A. Laskin, M.K. Gilles, P. Liu, A.M. Macdonald, J.W. Strapp and G.M. McFarquhar, 2013: Chemical characterization of individual particles and residuals of cloud droplets and ice crystals collected onboard research aircraft in the ISDAC 2008 study. *J. Geophys. Res.*, **118**, 6564-6579, doi:10.1002/jgrd.50484.

Jackson, R.C., G.M. McFarquhar, A.V. Korolev, M.E. Earle, P.S.K. Liu, R.P. Lawson, S. Brooks, M. Wolde, A. Laskin, and M. Freer, 2012: The dependence of ice microphysics on aerosol concentration in arctic mixed-phase stratus clouds during ISDAC and M-PACE. *J. Geophys. Res.*, **117**, D15, doi:10.1029/2012JD017668.

Jackson, R.C, G.M. McFarquhar, J. Stith, M. Beals, R. Shaw, J. Jensen, J. Fugal, and A. Korolev, 2014: An assessment of the impact of anti-shattering tips and artifact removal techniques on cloud ice size distributions measured by the 2D cloud probe. *J. Atmos. Ocean. Tech.*, **31**, 2567-2590.

Jackson, R.C., and G.M. McFarquhar, 2014: An assessment of the impact of anti-shattering tips and artifact removal techniques on bulk cloud ice microphysical and optical properties

measured by the 2D cloud probe. *J. Atmos. Ocean. Tech.*, **31**, 2131-2144.

Jackson, R.C, G.M. McFarquhar, A. Fridlind, and R. Atlas, 2015: The dependence of cirrus gamma size distributions expressed as volumes in N_0-λ–μ phase space and bulk cloud properties on environmental conditions: Results from the Small Ice Particles in Cirrus Experiment (SPARTICUS). *J. Geophys. Res.*, **120,** 10351-10377.

Lee, S.-S., C. H. Jung, C. Lee, B. G. Kim, J. Um , S. S. Yum, and H. Lee, 2014: Effects of aerosol on evaporation, freezing and precipitation in a multiple cloud system. *Earth Planet. Sci. Lett.,* accepted with minor revision.

Lim, K.-S. S., L. Riihimaki, S.A. McFarlane, J. Comstock, B. Schmidt, C. Sivaraman, Y. Shi, and G. McFarquhar, 2016: Variation of long-term surface-retrieved cloud-droplet number concentration with in situ aircraft observations. *J. Geophys. Res.*, Under review.

Lindqvist, H., K. Muinonen, T. Nousiainen, R. Makkonen, J. Um, P. Mauno, G.M. McFarquhar, and H. Hakkarainen, 2012: Ice-cloud particle habit classification with atmospheric radiation applications. *J. Geophys. Res.*, 117, D16206, doi:10.1029/2012JD017573.

Maahn, M., U. Lohnert, P. Kollias, R.C. Jackson, and G.M. McFarquhar, 2015: Developing and evaluating ice cloud parameterizations for forward modeling of radar moments using in situ aircraft observations. *J. Atmos. Ocean. Tech.*, **32,** 880-903.

McFarquhar, G.M., J. Um, and R. Jackson, 2013: Small particle shape in mixed-phase clouds. *J. Appl. Meteor. Clim.*, **52**, 1277-1293.

McFarquhar, G.M., T.-L. Hsieh, M. Freer, J. Mascio, and B.F. Jewett, 2015: The characterization of ice hydrometeor gamma size distributions as volumes in $N_0/\lambda/\mu$ phase space: implications for microphysical process modeling. *J. Atmos. Sci.*, **72**, 892-909.

Ovchinnikov, M., A. Ackerman, A. Avramov, A. Cheng, J. Fan, A. Fridlind, S. Ghan, J. Harrington, C. Hoose, A. Korolev, G. McFarquhar, H. Morrison, M. Paukert, J. Savre, B. Shipway, M. Shuppe, A. Solomon, and K. Sulia, 2013: Intercomparison of large-eddy simulations of Arctic mixed-phase clouds: Importance of ice size distribution assumptions. *J. Advances in Modeling Earth Systems*, 6, doi:10.1002/2013MS000282

Schmid, B., J.M. Tomlinson, J.M. Hubbe, J.M. Comstock, F. Mei, D. Chand, M.S. Pekour, C.D. Kluzek, E. Andrews, S.C. Biraud, and G.M. McFarquhar, 2014: The DOE ARM Aerial Facility. *Bull. Amer. Meteor. Soc.*, **95**, 723-742.

Schmid, B., G.M. McFarquhar, and R. Ellingson, 2015: ARM Aircraft Measurements (1993-2009). Monograph on DOE ARM Program for *Amer. Meteor. Soc.*, In press.

Um, J. and G.M. McFarquhar, 2009: Single-scattering properties of aggregates of plates, Q. J. Roy. Meteor. Soc., **135,** 291–304.

Um, J., and G.M. McFarquhar, 2013: Optimal numerical methods for determining the orientation average of single-scattering properties of ice crystals. *J. Quant. Spect. Rad. Trans.*, **127**, doi:10.1016/j.jqsrt.2013.05.020.

Um., J., and G.M. McFarquhar, 2015: Formation of atmospheric halos and applicability of geometric optics for calculating single-scattering properties of hexagonal ice crystals: Impacts of aspect ratio and crystal size. *J. Quant. Spec. Rad. Transfer*, 165, 134-152.

Um, J., G.M. McFarquhar, Y.P. Hong, S.-S. Lee, R.P. Lawson, and Q. Mo, 2015: Dimensions and aspect ratios of natural ice crystals in cirrus. *Atmos. Chem. Phys.,* 15, 3933-3956, doi:10.5194/acp-15-3933-2015.

Um, J., and G.M. McFarquhar, 2016a: The impacts of shapes and concentrations of small ice crystals on bulk scattering properties of tropical cirrus. *J. Geophys. Res.*, Under preparation.

Um J., and G. M. McFarquhar, 2016b: Accuracy of discrete-dipole approximation and T-matrix method in calculations of single-scattering properties of hexagonal particles. *J. Quant. Spectrosc. Radiat. Transfer,* in preparation.

Um, J., G.M. McFarquhar, T. Nousiainen, J. Tiira, H. Lindqvist, A. Schwarzenboeck, A. Delplanque, 2016a: Comparing the performance of habit identification algorithms for high resolution ice crystals. *J. Atmos. Ocean. Tech.*, In preparation.

Um, J., P.J. Connolly, G.M. McFarquhar, C. Emersic, Z.J. Ulanowski, and M. Gallagher, 2016b: A laboratory study to assess the performance of three generations of Cloud Particle Imagers, *J. Atmos. Ocean. Tech.*, In preparation (manuscript available).

Verlinde, J., M.P. Rambukkange, E.E. Clothiaux, G.M. McFarquhar, and E.W. Eloranta, 2013: Arctic multi-layered mixed-phase cloud processes revealed in Doppler spectra. *J. Geophys. Res.*, 118, doi: 10.1002/2013JD020183.

Vogelmann, A.M., G. McFarquhar, J. Ogren, D. Turner, J. Comstock, G. Feingold, C. Long, H. Jonsson, A. Bucholtz, D. Collins, G. Diskin, H. Gerber, P. Lawson, R. K. Woods, E. Andrews, H.-J. Yang, J.C. Chiu, D. Harstock, J. Hubbe, C. Lo, A. Marshak, J.W. Monroe, S.A. McFarlane, B. Schmid, J.M. Tomlinson, and T. Toto, 2012a: RACORO extended-term, aircraft observations of boundary layer clouds. *Bull. Amer. Meteor. Soc.,* **93**, 861-878.

Wu, W., and G.M. McFarquhar, 2016a: On the practical definitions of maximum dimension for non-spherical particles recorded by 2D probes. *J. Atmos. Ocean. Tech.*, Under review.

Wu, W., and G.M. McFarquhar, 2016b: Dependence of cloud properties on environmental conditions: results from MC3E. *Atmos. Chem. Phys..*, to be submitted.

Yang, H.-J., and G.M. McFarquhar, 2012: Effects of aerosols on shallow cumuli sampled during RACORO. *16th Int. Conf. Clouds Precip.*, Leipzig, Germany, 28 July to 3 August 2012.

Yang, H.-J., and G.M. McFarquhar, 2016: Aerosol-cloud interactions in shallow cumuli during RACORO. *J. Atmos. Sci.*, In preparation.

Zamora, L.M., R.A. Kahn, B.E. Anderson, E. Apel, G.S. Diskin, J.-L. Jimenez, G.M. McFarquhar, A. Nenes, A. Wisthaler, Y. Kondo, A. Zelenyuk-Imre, and L. Ziemba, 2015: Aircraft-measured indirect cloud effects from biomass burning smoke in the Arctic and subarctic. *Atmos. Chem. Phys. Disc.*, Under review

Conference Proceedings & Presentations and Papers in Preparation:

Atlas, R., A.M. Fridlind, E.J. Moyer, P. Lawson, G.M. McFarquhar, J. Um, G. Diskin, and H. Kalesse, 2013: Using SPartICus measurements to study ice particle size distribution modes within in situ cirrus. *American Geophysical Union Fall Meeting*, San Francisco, CA, December 2013.

Atlas, R., A. Fridlind, E. Moyer, P. Lawson, and G. McFarquhar, 2014: Using SPartICus measurements to study the occurrence and source of ice particle size distribution features in mid-latitude synoptic cirrus. *14th Amer. Meteor. Soc. Conference on Cloud Physics*, Boston, MA.

Baumgardner, D., A. Heymsfield, G. McFarquhar and D. Cziczo, 2014: Challenges in analyzing and presenting cloud microphysical data measured with airborne cloud probes. 14th Amer. Meteor. Soc. Conference on Cloud Physics, Boston, MA.

Earle, M.E., P.S.K. Liu, J.W. Strapp, G.M. McFarquhar, A. Zelenyuk, D. Imre, M. Ovchinnikov, N.C. Shantz, S.J. Ghan, and W.R. Leaitch, 2012: Droplet closure analysis of arctic stratocumulus clouds during ISDAC. *3rd Science Team Meeting of Atmospheric System Research (ASR) Program*, Arlington, VA, 12 to 16 March 2012.

Endo, S., A.M. Fridlind, W. Lin, A.M. Vogelmann, T. Toto, A.S. Ackerman, G.M. McFarquhar, R.C. Jackson, H.H. Jonsson, and Y. Liu, 2015: RACORO continental boundary layer cloud investigations: Large-eddy simulations of cumulus clouds and evaluation with in-situ and ground-based observations. Fall Meeting American Geophysical Union, San Francisco, CA.

Fridlind, A., R. Atlas, J. Um, G. McFarquhar, A.S. Ackerman, B. van Diedenhoven, E.J. Moyer, and P. Lawson, 2014: Derivation and testing of consistent physical and optical properties of mid-latitude cirrus ice crystals for a size-resolved microphysics model. 14th Amer. Meteor. Soc. Conference on Cloud Physics, Boston, MA.

Fridlind, A., A. Ackerman, X. Li, W.-K. Tao, M. van Lier-Walqui, D. Wu, X. Dong, G. McFarquhar, A. Ryzhkov, J. Wang, and W. Wu, 2015: MC3E studies of deep convection

updraft and outflow microphysics: NU-WRF with bin and bulk microphysics versus observations. Atmos. Sys. Res. Program Annual Meeting, Vienna, VA

Fridlind, A.M., A.S. Ackerman, A. Schwarzenboeck, W. Strapp, A. Korolev, M. van Lier-Walqui, G. McFarquhar, W. Wu, and C. Williams, 2015: Use of observations and simulations to investigate primary microphysical pathways between deep convection updrafts and the stratiform melting level. IUGG Symposium, Prague, Czech Republic, June-July 2015.

Haapanala, P., G. McFarquhar, A. Macke, P. Raisanen, M. Kahnert, and T. Nousiainen, 2014: Dependence of circumsolar radiation on ice cloud properties. 14th Amer. Meteor. Soc. Conference on Cloud Physics, Boston, MA.

Haapanala, P., G.M. McFarquhar, J. Um, and T. Nousiainen, 2016: Simulation of multi-directional radiances using microphysical data collected in mid-latitude cirrus: comparison against direct observations of radiative flux. *J. Atmos. Sci.*, In preparation.

Hsieh, T.-L., G. McFarquhar, and M. Freer, 2012: An intercomparison of techniques used to fit gamma distributions to cloud particle size distributions. *11th Amer. Meteor. Soc., Student Conf. and Career Fair*, New Orleans, LA, 22 January 2012.

Jackson, R.C., G.M. McFarquhar, J. Stith, and J. Jensen, 2012: A comparison of bulk ice microphysical properties derived using 2D cloud probes with and without shatter reducing tips and correction algorithms. *16th Int. Conf. Clouds Precip.*, Leipzig, Germany, 28 July to 3 August 2012.

Jackson, R.C., G.M. McFarquhar, J. Stith, D.C. Rogers, and W.A. Cooper, 2012: Resolving uncertainties in climate prediction by improving the treatment of small ice particles. *Lower Atmospheric Facilities Observing Workshop*, Boulder, CO, June 2012.

Jackson, R., G.M. McFarquhar, and R.P. Lawson, 2014: The relationship between cirrus ice microphysical properties and meteorological conditions observed during SPARTICUS. *5th ASR Science Team Meeting,* U.S. Department of Energy, Potomac, MD, USA.

Jackson, R., G.M. McFarquhar, and R.P. Lawson, 2014: The relationship between cirrus ice microphysical properties and meteorological conditions observed during SPARTICUS. 14th Amer. Meteor. Soc. Conference on Cloud Physics, Boston, MA.

Korolev, A., M. Ovchinnikov, and G. McFarquhar, 2012: Characterizing the structure of persistent mixed-phase Arctic clouds during ISDAC using in-situ observations and modeling. *International Polar Year Conference*, Montreal, Canada, 22-27 April 2012.

McFarquhar, G.M., and J. Um, 2012: Quantifying and reducing uncertainty in observed sizes, shapes and concentrations of small ice crystals: Implications for derived scattering properties at visible wavelengths. *International Radiation Symposium*, Berlin, Germany, 6 to 10 August 2012.

Maahn, M., U. Loehnert, P. Kollias, R. Jackson, and G. McFarquhar, 2015: Using higher radar moments to study ice clouds with vertically pointing cloud radars. Atmos. Sys. Res. Program Annual Meeting, Vienna, VA

McFarquhar, G., R. Jackson, A. Korolev, M. Earle, P. Liu, P. Lawson, S. Brooks, M. Wolde, A. Laskin, and M. Freer, 2012: The dependence of arctic mixed-phase stratus ice cloud microphysics on aerosol concentration using observations acquired during ISDAC. *3rd Science Team Meeting of Atmospheric System Research (ASR) Program*, Arlington, VA, 12 to 16 March 2012.

McFarquhar, G.M., T.-L. Hsieh, M. Freer, and B.F. Jewett, 2012: The characterization of hydrometeor size distributions fit to gamma functions as surfaces in $N_0/\lambda/\mu$ phase space: implications for microphysical process rates. *16th Int. Conf. Clouds Precip.*, Leipzig, Germany, 28 July to 3 August 2012.

McFarquhar, G.M., R.C. Jackson, A.V. Korolev, J.W. Strapp, M.E. Earle, P.S.K. Liu, A. Laskin, R.P. Lawson, S. Brooks, and M. Freer, 2012: The dependence of single-layer arctic stratus ice microphysical properties on aerosol properties observed during ISDAC and M-PACE. *16th Int. Conf. Clouds Precip.*, Leipzig, Germany, 28 July to 3 August 2012.

McFarquhar, G.M., 2013: In-situ measurements of cloud microphysics from M-PACE and ISDAC: what additional observations from UAS can provide, Planning and Operational Meeting on Polar Atmospheric Measurements Related to DOE ARM Program using small Unmanned Aerial Systems and Tethered Balloons, Washington, DC, July 2013.

McFarquhar, G.M., 2013: The physics of clouds: how aircraft observations improve our knowledge of clouds for weather and climate studies. *80th Annual Meeting of the Southern Eastern Branch of the American Physical Society*, Bowling Green, KT, November 2013.

McFarquhar, G.M., R. McCoy, A. Vogelmann, J. Um, and H.-J. Yang, 2013: Measurements of cloud and radiative properties from piloted aircraft using an RPA-type approach, First Conference of the International Society for Atmospheric Research using Remotely Piloted Aircraft (ISARRA) 2013, Palma de Mallorca, Spain.

McFarquhar, G.M., J. Buhl, W. Wobrock, 2013: Ice/liquid partitioning in mixed-phase cloud. *Workshop on Measurement Problems in Ice Clouds*, International Commission on Clouds and Precipitation, Zurich, Switzerland, July 2013.

McFarquhar, G.M., J. Um, T.-L. Hsieh, M. Freer, B.F. Jewett, J. Mascio, S.K. Kim, K. Yaffe, T. Nousiainen, J. Tiira, H. Lindqvist, A. Schwarzenboeck, and A. Delplanque, 2013: Use of in-situ cloud probe data to derive bulk cloud parameters and their uncertainties: Impacts for models and remote sensing retrievals. *American Geophysical Union Fall Meeting*, San Francisco, CA, December 2013.

McFarquhar, G. M., J. Um, S. K. Kim, K. Yaffe, W. Wu, and T. L. Hsieh, 2013: Aspect ratios, habit classifications, and size distributions of ice crystals: construction of a database for arctic, tropical and mid-latitude clouds. *ASR Fall Working Group Meeting*, U.S. Department of Energy, Rockville, MD, USA.

McFarquhar, G.M., and J. Um, 2014: The impact of natural variations of ice crystal aspect ratios on single-scattering radiative properties. 14th Amer. Meteor. Soc. Conference on Atmos. Rad., Boston, MA.

McFarquhar, G.M., J. Buhl, W. Wobrock, O. Jourdan, and M. Hamilton, 2014: Ice/liquid mass partitioning in mixed phase clouds: current knowledge, uncertainties and challenges, Monograph for *Amer. Meteor. Soc.* on Measurement Uncertainties in Ice-phase clouds, In preparation.

McFarquhar, G.M., T.-L. Hsieh, M. Freer, J. Mascio, and B. Jewett, 2014: The characterization of ice hydrometeor gamma size distributions as volumes in $N0/\lambda/\mu$ phase space: implications for microphysical process modeling. 3rd Annual Meeting of Atmosphere Systems Research Science Team, Potomac, MD.

McFarquhar, G.M., R. Jackson, J. Stith, M. Beals, R. Shaw, J. Jensen, J. Fugal, and A. Korolev, 2014: The impact of shattering on derived microphysical parameters from optical array probes: results from ISDAC and IDEAS-2011. 14th Amer. Meteor. Soc. Conference on Atmos. Rad., Boston, MA.

McFarquhar, G.M., T.-L. Hsieh, M. Freer, J. Mascio, and B.F. Jewett, 2014: How estimates of uncertainty in measured particle size distributions can be used to characterize the variability of gamma/exponential functions used in numerical models. 14th Amer. Meteor. Soc. Conference on Cloud Physics, Boston, MA.

McFarquhar, G.M., R. Jackson, W. Wu, J. Dong, T.-L. Hsieh, M. Freer, and S. Chu, 2015: Analysis of uncertainties in ice crystal size distributions, their representation as gamma distributions, and bulk properties derived from in-situ measurements during ARM field campaigns. Atmos. Sys. Res. Program Annual Meeting, Vienna, VA

Ovchinnikov, M., A. Ackerman, A. Avramov, G. de Boer, A. Fridlind, J. Harrington, S. Ghan, A. Korolev, A. Lock, G. McFarquhar, H. Morrison, B. Shipway, and M. Shupe, 2012: ISDAC LES intercomparison: Case setup and preliminary results. *3rd Science Team Meeting of Atmospheric System Research (ASR) Program*, Arlington, VA, 12 to 16 March 2012.

Ovchinnikov, M., A. S. Ackerman, A. Avramov, A. Cheng, J. Fan, A.M. Fridlind, J. Harrington, C. Hoose, S. Ghan, A. Korolev, G.M. McFarquhar, H. Morrison, M. Paukert, J. Savre, B.J. Shipway, M.D. Shupe, A. Solomon, and K. Sulia, 2014: Intercomparison of large-eddy simulations of Arctic mixed-phase clouds: Importance of ice size distribution assumptions. 5th Annual Meeting of Atmosphere Systems Research Science Team, Potomac, MD.

Tao, W.-K., D. Wu, X. Li, A. Fridlind, S. Lang, A. Ackerman, X. Dong, J. Wang, G. McFarquhar, and W. Wu, 2014: High-resolution model simulations of MC3E deep convective-precipitation systems: Comparison with radar and aircraft in-situ measurements. 3rd Annual Meeting of Atmosphere Systems Research Science Team, Potomac, MD.

Um, J., and G.M. McFarquhar, 2012: Optimal numerical methods for determining the orientation average of single-scattering properties of atmospheric ice crystals. *International Radiation Symposium*, Berlin, Germany, 6 to 10 August 2012.

Um, J., and G.M. McFarquhar, 2012: Single-scattering properties of small atmospheric ice crystals at absorbing wavelengths: Dependence on idealized models. *International Radiation Symposium*, Berlin, Germany, 6 to 10 August 2012.

Um, J., and G.M. McFarquhar, 2012: The dependence of the single-scattering properties of small ice crystals on orientation average, particle shape and wavelength. *Amer. Geophys. Union Fall Meeting*, December 2012.

Um, J., G.M. McFarquhar, P.J. Connolly, C. Emersic, Z. Ulanowski, and M. Gallagher, 2012: Calibration of three generations of Cloud Particle Imagers (CPIs) to improve measurements of particle size distributions. *16th Int. Conf. Clouds Precip.*, Leipzig, Germany, 28 July to 3 August 2012.

Um, J., 2013: Uncertainties in microphysical and scattering properties of ice clouds. Yonsei University, Seoul, Republic of Korea (Invited).

Um, J., 2013: Scattering properties of atmospheric ice crystals. Gangneung-Wonju National University, Gangneung, Republic of Korea (Invited).

Um, J., 2013: Light scattering by of atmospheric particles. Ewha Womans University, Seoul, Republic of Korea (Invited).

Um, J. and G. M. McFarquhar, 2014: Influences of orientation averaging scheme on the scattering properties of atmospheric ice crystals: Applications to atmospheric halo formation. *2nd Annual NCSA Blue Waters Symposium,* Champaign, IL.

Um J., and G. M. McFarquhar, 2014: Aspect ratios of natural crystals in ice clouds. *ASR Science Team Meeting,* U.S. Department of Energy, Potomac, MD, USA.

Um, J., and G.M. McFarquhar, 2014: Formation of atmospheric halos by hexagonal ice crystals. 14th Amer. Meteor. Soc. Conference on Atmos. Rad., Boston, MA.

Um, J., and G.M. McFarquhar, 2014: Aspect ratios of natural ice crystals derived from high-resolution images: dependence on environmental conditions. 14th Amer. Meteor. Soc. Conference on Cloud Physics, Boston, MA.

Um., J., and G.M. McFarquhar, 2015: Single particle database of natural ice crystals acquired during TWP-ICE, ISDAC, and SPARTICUS. Atmos. Sys. Res. Program Annual Meeting, Vienna, VA, March 2015.

Um, J., and G.M. McFarquhar, 2015: Applicability of geometric optics method for calculations of single-scattering properties of atmospheric ice crystals. Blue Waters Symposium, Third Annual NCSA Blue Waters Symposium for Petascale Science and beyond, Sunriver, OR, May 2015.

Um, J., and G.M. McFarquhar, 2015: A lower limit of applicability of the conventional geometric optics method: A comparison with the discrete dipole approximation for the scattering properties of atmospheric ice particles. XSEDE Science Conference, St. Louis, MO, July 2015

van Lier-Walqui, M., A. M. Fridlind, A.S. Ackerman, C. R. Williams, J. Wang Sr., X. Dong, W. Wu, G. McFarquhar, A. Grandin, F. Dezitter, J.W. Strapp, and A. Korolev, 2014: Use of S-band profiling radar and in-situ size distribution measurements to probabilistically constrain ice sticking efficiencies. *Fall Meeting of American Geophysical Union*, San Francisco, CA, December 2014.

van Lier-Walqui, M., A. Ackerman, C. Williams, G. McFarquhar, X. Dong, W. Wu, J. Wang, A. Korolev, A. Grandin, and W. Strapp, 2015: Bayesian estimation of ice sticking efficiency using profiling radar Doppler spectra and in-situ ice properties. Amer. Meteor. Soc. 37th Conference on Radar Meteorology, 14-18 September 2015, Norman, OK.

Vogelmann, A., T. Toto, M. Jensen, W. Lin, C. Lu, G. McFarquhar, R. Jackson, H. Jonsson, and Y. Liu, 2012: RACORO aircraft data case study development for FASTER. *3rd Science Team Meeting of Atmospheric System Research (ASR) Program*, Arlington, VA, 12 to 16 March 2012.

Vogelmann, A., T. Toto, W. Lin, Y. Liu, C. Lu, M. Jensen, G. McFarquhar, R. Jackson, and H. Jonsson, 2012: RACORO Aircraft data case study development for FASTER. *Pan-GCSS Meeting*, Boulder, CO, September 2012.

Vogelmann, A.M., T. Toto, W. Lin, Y. Liu, M.P. Jensen, C. Lu, G.M. McFarquhar, R. Jackson and H. Jonsson, 2012: RACORO aircraft data case study development for FASTER. *Amer. Geophys. Union Fall Meeting*, December 2012.

Vogelmann, A., A. Fridlind, T. Toto, S. Endo, W. Lin, Y. Liu, G. McFarquhar, R. Jackson, and J. Wang, 2014: RACORO-FASTER case study generation for continental boundary layer clouds. 3rd Annual Meeting of Atmosphere Systems Research Science Team, Potomac, MD.

Vogelmann, A., A. Fridlind, S. Endo, W. Lin, T. Toto, Y. Liu, J. Wang, G. McFarquhar, R. Jackson, Z. Li, S. Feng, A. Ackerman, M. Zhang, S. Xie and Y. Zhang, 2014: RACORO-

FASTER case studies for continental boundary layer clouds. *7th Int. Scientific Conf. Global Water and Energy Cycle*, Montreal, QC, August 2014.

Vogelmann, A. Fridlind, T. Toto, S. Endo, W. Lin, Y. Liu, J. Wang, S. Feng, Y. Zhang, D. Turner, A. Ackerman, G. McFarquhar, R. Jackson, Z. Li, S. Xie, M. Zhang, and M. Khairoutdinov, 2015: RACORO case sutides of continental boundary layer clouds. Atmos. Sys. Res. Program Annual Meeting, Vienna, VA

Wendisch, M., M. Kramer, C. Franklin, G.M. McFarquhar, R.P. Lawson, D. Cziczo, K. Sassen, P. Minnis, and Alexander, 2014: Cirrus formation, evolution and impact on climate. Monograph for *Amer. Meteor. Soc.* on Measurement uncertainties in ice clouds, In preparation.

Wu, W., and G.M. McFarquhar, 2014: The impact of varying definitions of particle maximum dimension on calculations of cloud properties from optical imaging probe data. 3rd Annual Meeting of Atmosphere Systems Research Science Team, Potomac, MD.

Wu, W., and G.M. McFarquhar, 2014: The meaning and significance of the definition of ice crystal maximum dimension: impacts on calculated cloud properties from two-dimensional particle images. 14th Amer. Meteor. Soc. Conference on Cloud Physics, Boston, MA.

Wu, W., and G.M. McFarquhar, 2015: Contrasting ice microphysical properties of wintertime frontal clouds and summertime convective clouds. Fall Meeting, Amer. Geophysical Union, San Francisco, CA.

Yang, H.-J., R. Rauber and G. McFarquhar, 2014: Aerosol-cloud interactions in shallow cumuli: meteorology versus aerosol. 14th Amer. Meteor. Soc. Conference on Cloud Physics, Boston, MA.

Yang, H.-J., R. M. Rauber, and G.M. McFarquhar, 2015: The impacts of aerosols and boundary layer characteristics on the properties of continental shallow cumuli during RACORO. Amer. Meteor. Soc. Annual Meeting, Phoenix, AZ, January 2015.

Zamora, L.M., R. Kahn, B. Anderson, G. McFarquhar, A. Wisthaler, and A. Zelenyuk, 2014: Indirect cloud effects from biomass burning smoke in the arctic and subarctic: insights from multiple in-situ studies. Fall Meeting of American Geophysical Union, San Francisco, CA, December 2014.

Zamora, L.M., R. Kahn, B. Anderson, G. McFarquhar, A. Wisthaler, and A. Zelenyuk, 2015: Polar clouds, precipitation and aerosols. Canadian Meteorological and Oceanographic Society.

Table 1. Ice crystal habit classification for SPARTICUS data. For flights indicated with blue are that all habit classification were completed, whereas those with red are completed for columns, plates, and bullet rosettes only.

January	February	March	April	June
0119A	0211B	0322A	0401A	0611A
0120A		0323A	0401B	0612A
0120B		0330A	0402A	0614
		0330B	0411A	0615A
			0411B	0624A
			0414B	
			0422B	
			0424A	
			0428A	
			0428B	
			0429	

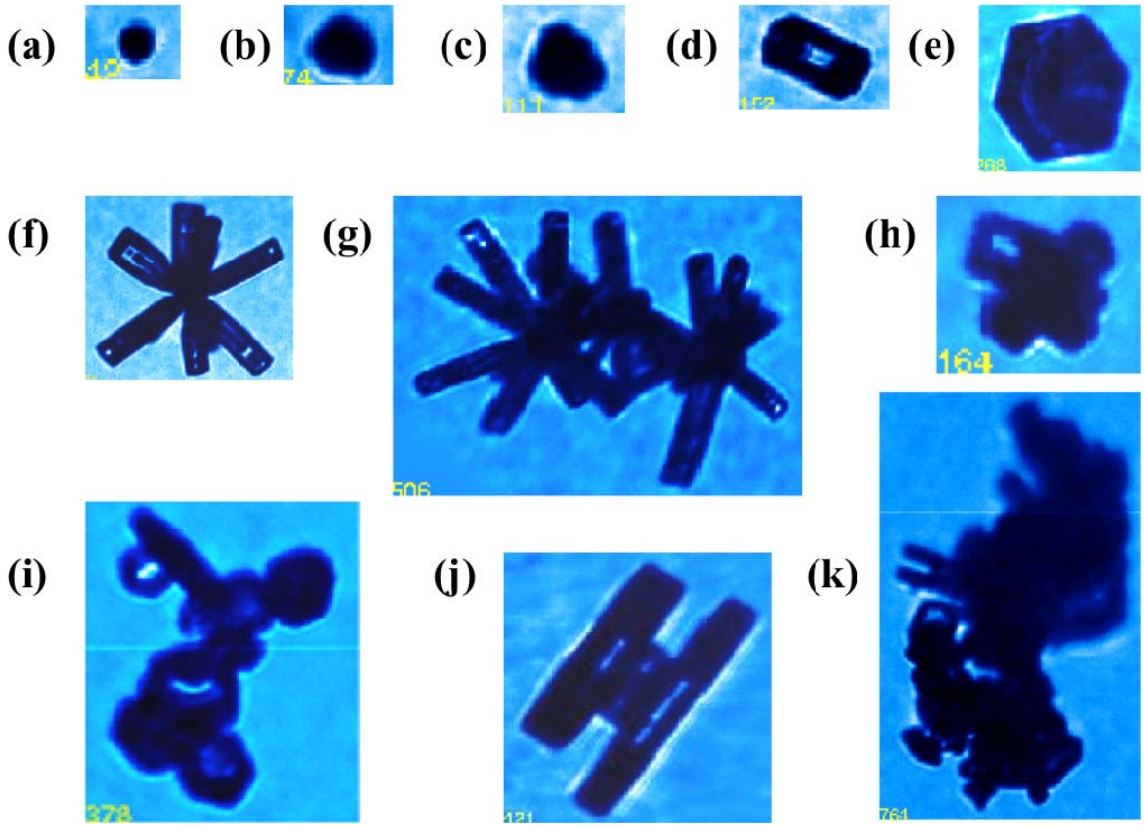

Figure 1: CPI images of shapes in classification algorithm: (a) small quasi-sphere (SQS), (b) medium quasi-sphere (MQS), (c) large quasi-sphere (LQS), (d) column (COL), (e) plate (PLT), (f) bullet rosette (BR), (g) aggregates of bullet rosettes (ABRs), (h) aggregates of columns (ACs), (i) aggregates of plates (APs), (j) capped column (CC), and (k) unclassified (UC).

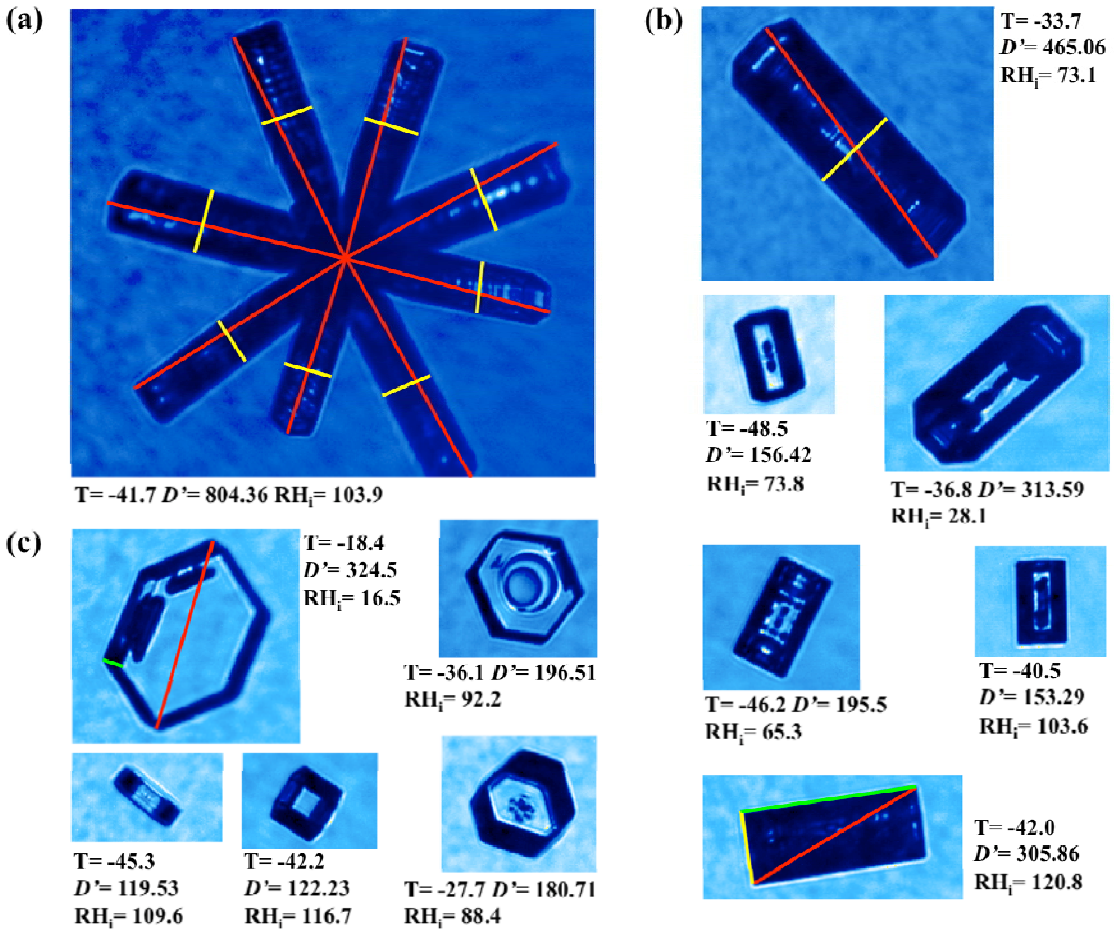

Figure 2: Example CPI images of ice crystals of (a) bullet rosette, (b) columns, and (c) plates taken during SPARTICUS. The projected maximum dimension (*D'*, red), projected width (*W'*, yellow), and projected length (*L'*, green) are specified in the first crystal in each panel. In each crystal, temperature (T, °C), projected maximum dimension (*D'*, μm), and relative humidity respect to ice (RH_i, %) are indicated. For columns upper three images are columns with orientations, whereas lower three are horizontally oriented respect to imaging plane.

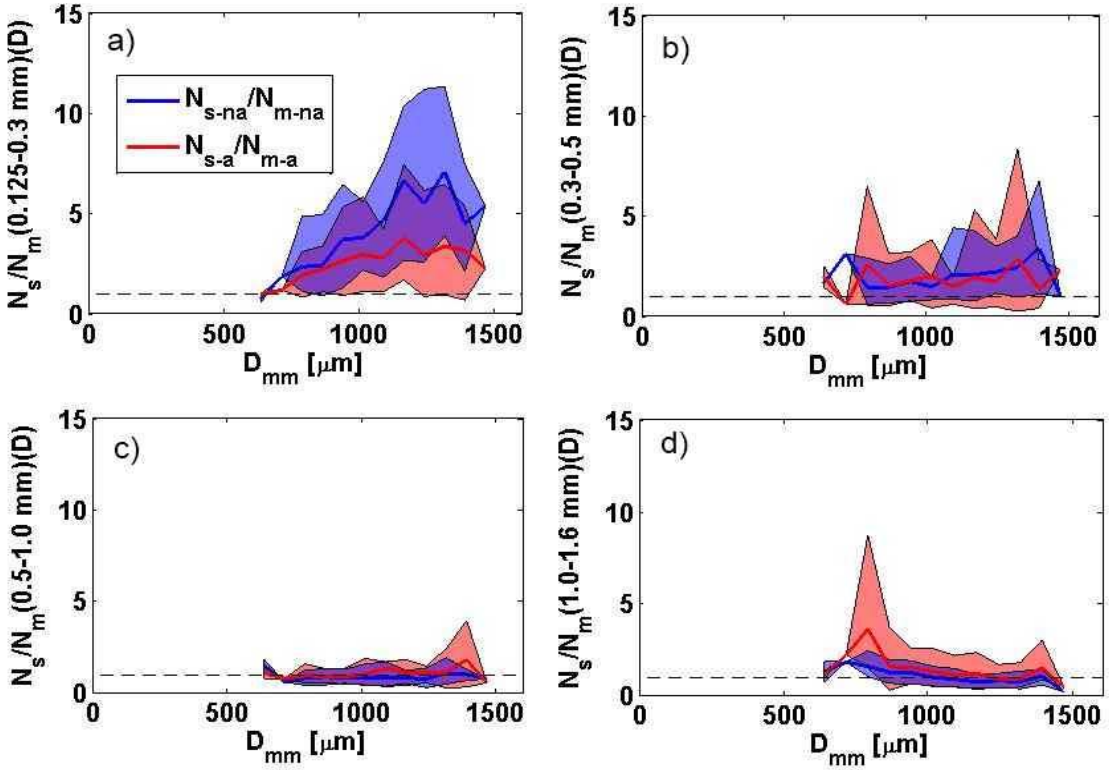

Figure 3: N_s/N_m for **(a)** 125 < D < 300 μm, **(b)** 300 < D < 500 μm, **(c)** 500 < D < 1000 μm, **(d)** 1000 < D < 2000 μm as a function of D_{mm} for two sorties flown 30 Apr 2008 during ISDAC when probes with conventional and anti-shattering tips were installed adjacent to each other on the National Research Council of Canada Convair-580. Solid lines denote means, width of shading denote 10th and 90th percentiles. Blue shading and lines denote N_s/N_m calculated without use of both shattered artifact removal algorithms. Red shading and line denote N_s/N_m calculated with use of both shattered artifact removal algorithms.

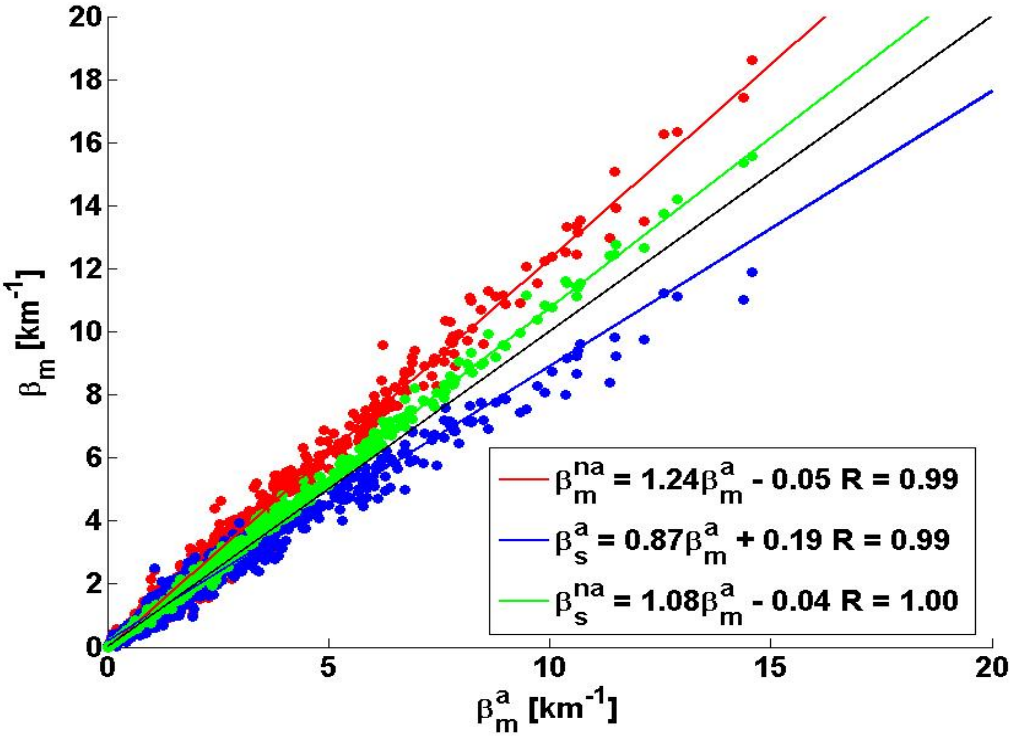

Figure 4: Scatter plot of β_s^{na}, β_s^a, and β_m^{na} as a function of β_m^a for ISDAC and IDEAS-2011. Solid lines are best fit of quantity on *y* axis to quantity on *x* axis.

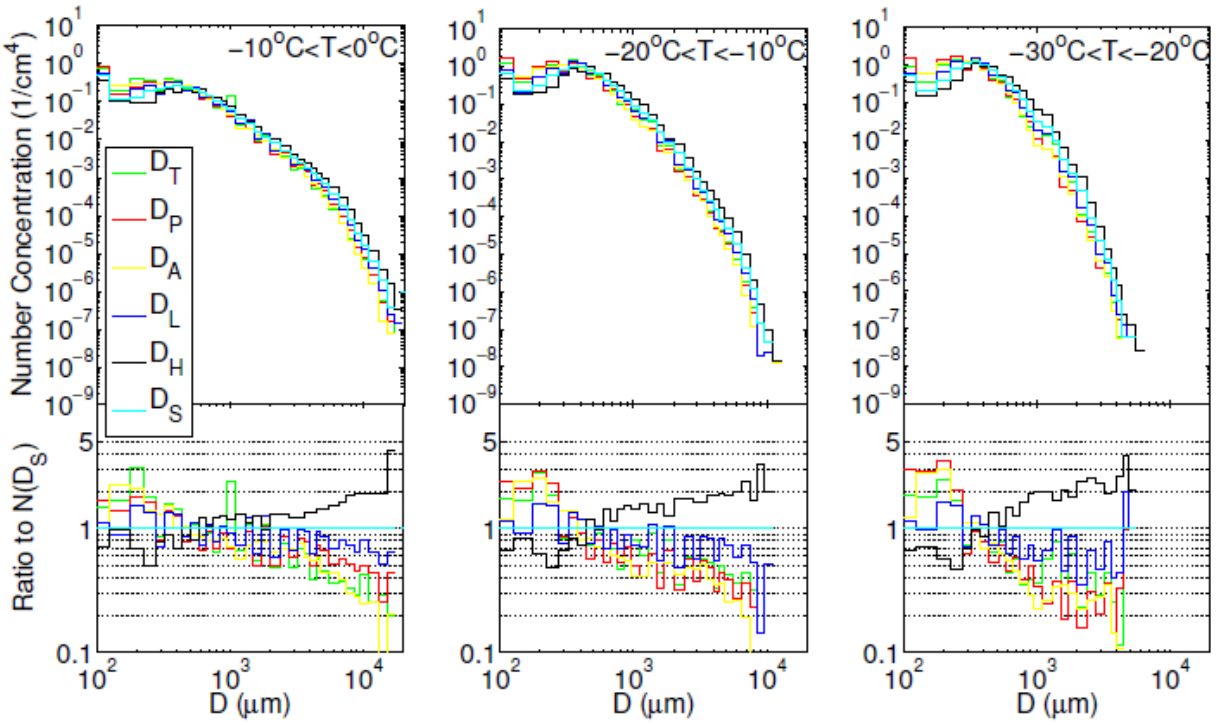

Figure 5: (upper panels) Number distribution function as function of D_{max} derived using in-situ data collected during MC3E on 20 May 2011, with different lines corresponding to SDs derived using different definitions of D_{max}. Different panels correspond to measurements made in different temperature range. (lower panels) Ratio of number distribution function using alternate definitions of D_{max} to that obtained using the diameter of the smallest enclosing circle about the particle (D_s) derived using the algorithm described by Wu and McFarquhar (2016a).

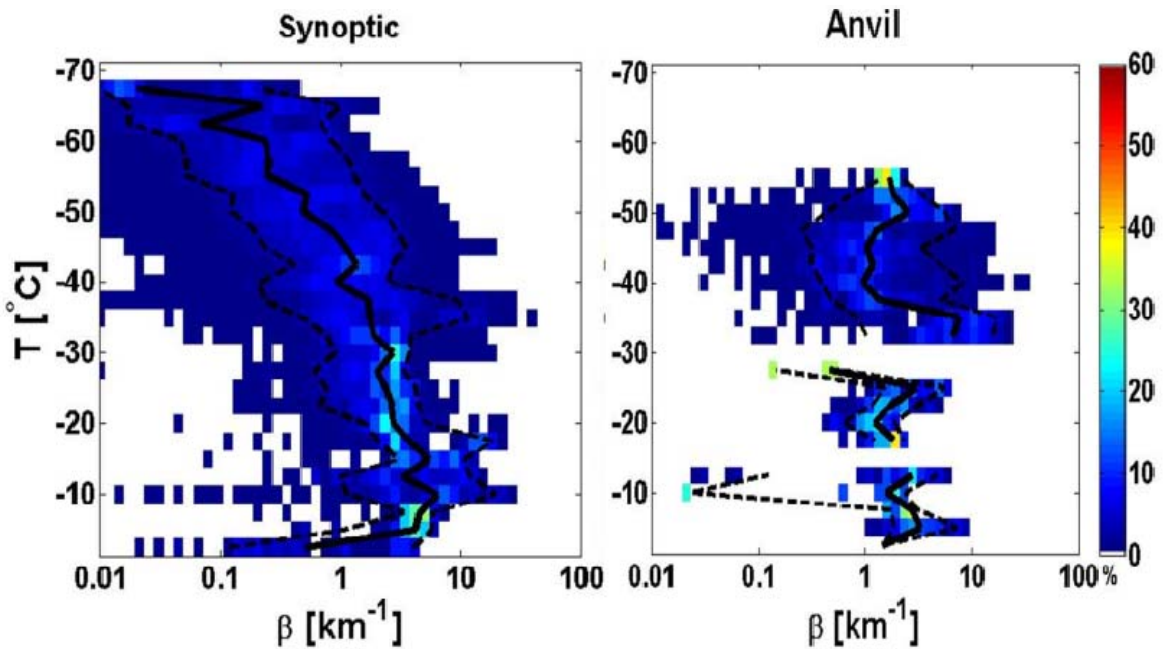

Figure 6: Frequency of β normalized by temperature T for synoptically (left) and convectively generated cirrus (right). Black line = median. Dashed lines = 10th/90th percentiles.

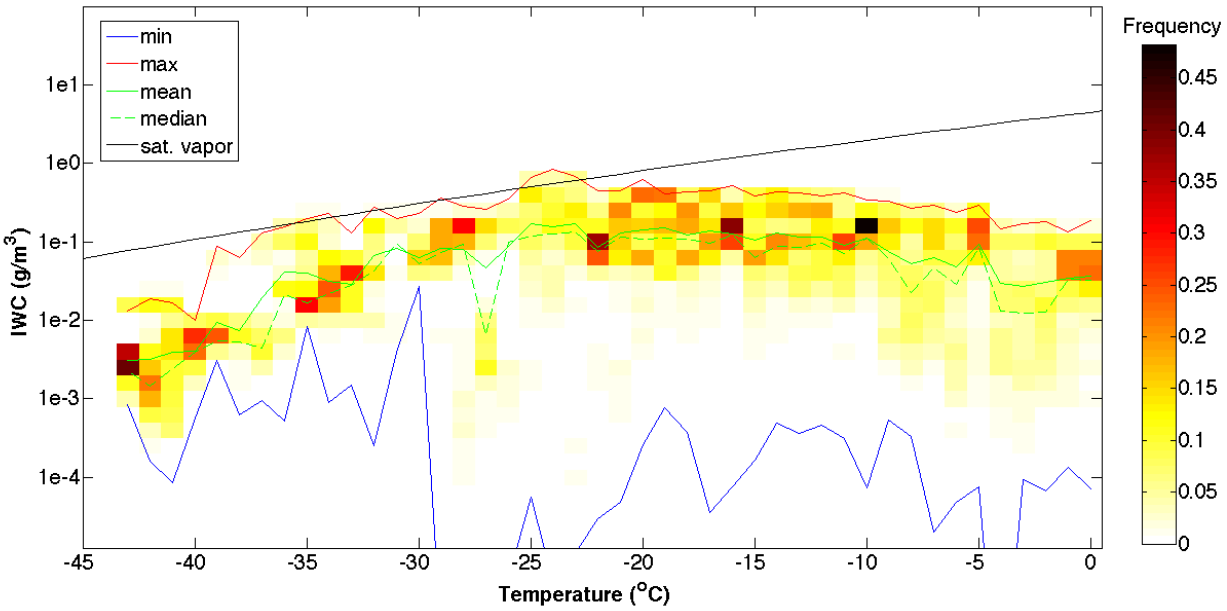

Figure 7: Frequency of *IWC* normalized by temperature *T* using data collected during 4 flights during MC3E (18, 20, 23 and 24 May 2011). The black line represents the median of the distribution, the blue line represents the lower quartile and the red line the upper quartiles.

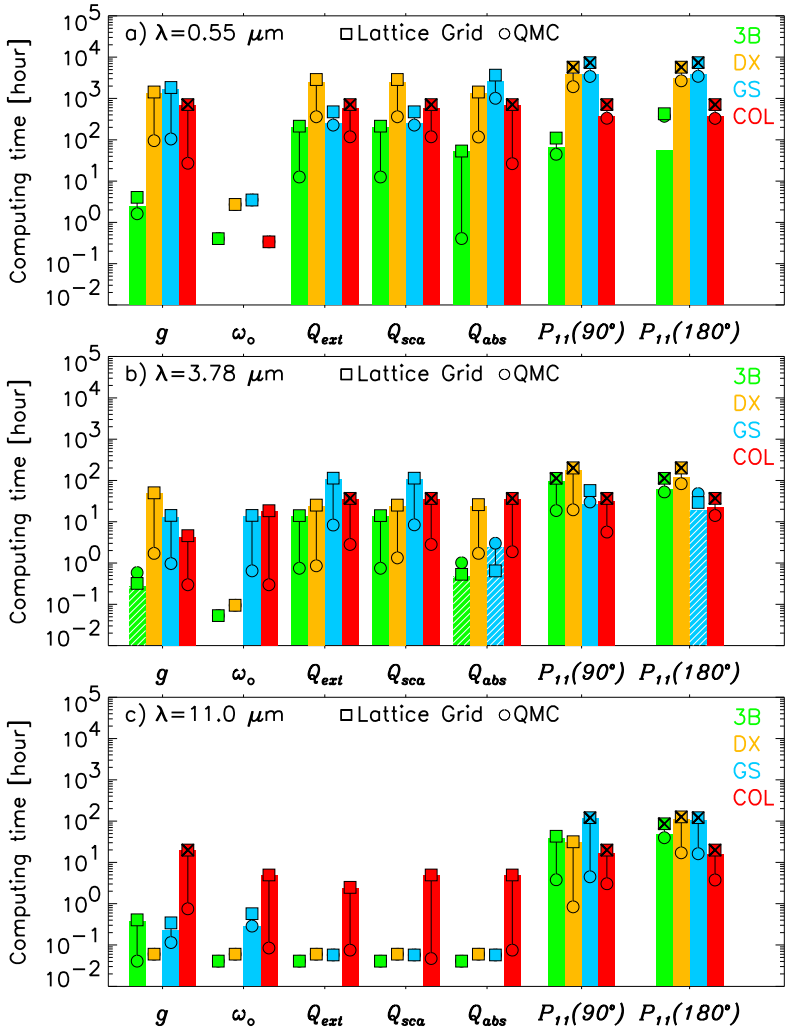

Figure 8: The computing time (in hours) required to achieve 1.0% accuracy in single-scattering properties (g, ω_o, Q_{ext}, Q_{sca}, Q_{abs}, P_{11} (90°), and P_{11} (180°)) using the lattice grid (square) and using the QMC (circle) at (a) λ=0.55 μm, (b) λ=3.78 μm, and (c) λ= 11.0 μm as determined using 300 2.6 GHz CPUs. Differences in computing time (lattice grid - QMC) are also shown with bar plots. Solid filled color bars indicate positive differences (computing time using lattice grid > QMC), whereas negative differences (computing time using lattice grid < QMC) are shown as striped pattern color bars. Different ice crystal models (i.e., 3B, DX, GS, and COL) are indicated with different colors. The computing time of non-converging single-scattering properties using the lattice grid are indicated with an X inside the square.

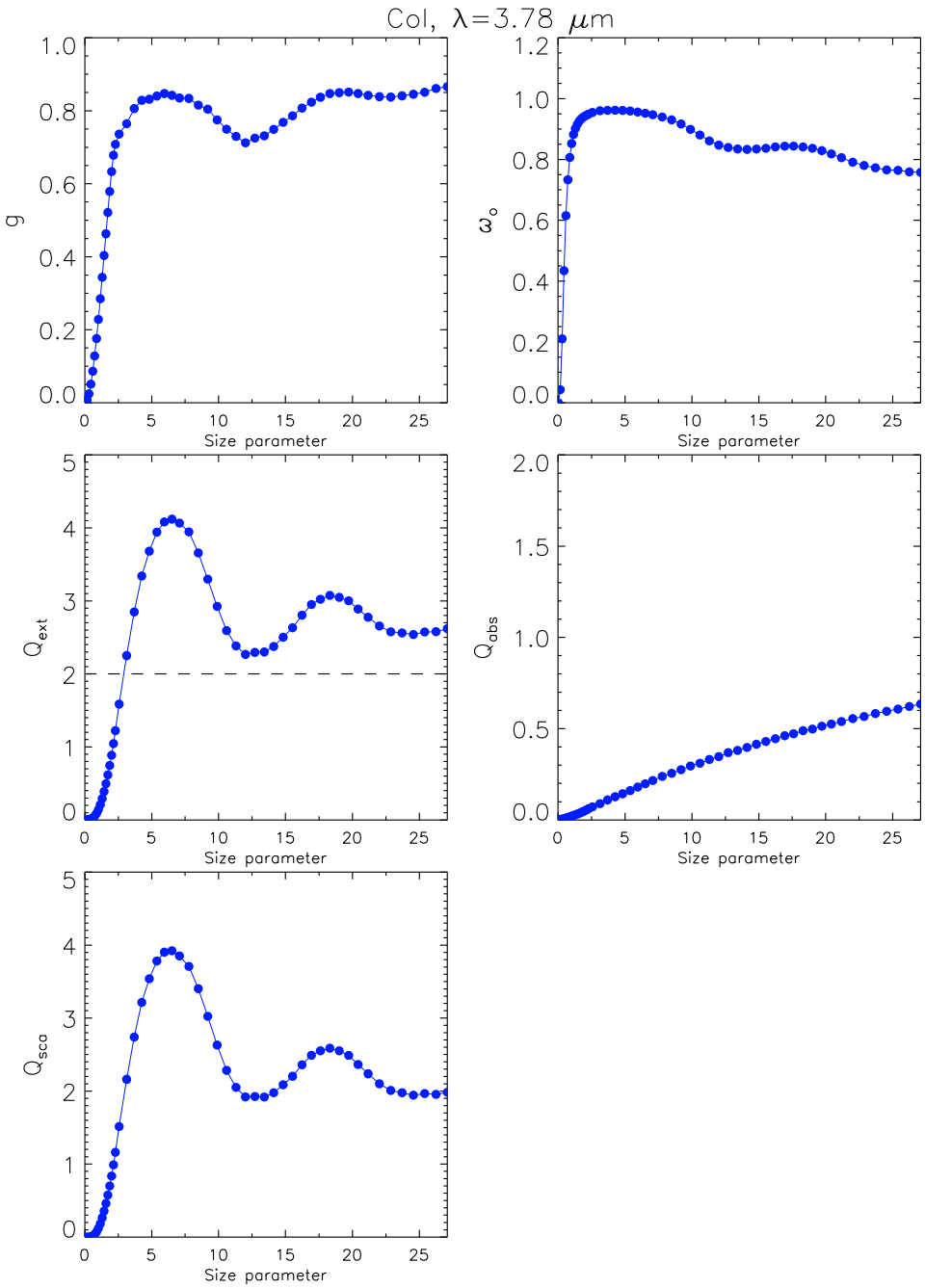

Figure 9. Calculated single-scattering properties of a column at λ=3.78 μm as a function of a size parameter. From left top to clockwise asymmetry parameter (g), single-scattering albedo (ω_o), absorption efficiency (Q_{abs}), scattering efficiency (Q_{sca}), and extinction efficiency (Q_{ext}).

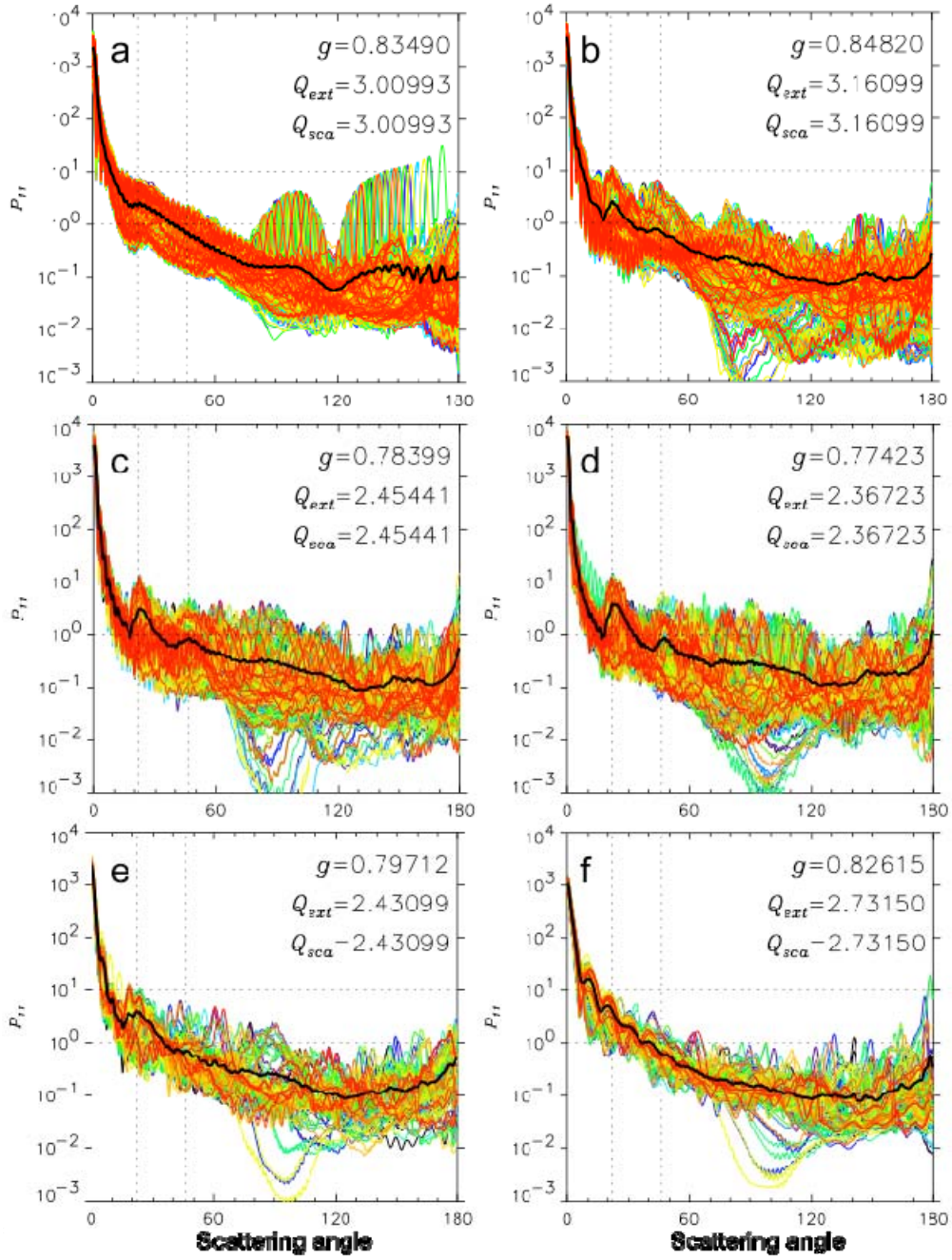

Figure 10: The scattering phase function P_{11} of six different aspect ratio (AR) of hexagonal ice crystals with D=16 μm: (a) L=1.6 μm, W=16.0 μm, and AR=0.1, (b) L=4.0 μm, W=16.0 μm, and AR=0.25, (c) L=8.0 μm, W=16.0 μm, and AR=0.5, (d) L=16.0 μm, W=16.0 μm, and AR=1.0, (e) L=16.0 μm, W=8.0 μm, and AR=2.0, and (f) L=16.0 μm, W=4.0 μm, and AR=4.0. The black line in each panel indicates orientation averaged P_{11}, whereas other color lines are P_{11} of each orientation. The g, Q_{ext}, and Q_{sca} are also shown. The scattering angles of 22° and 46° are indicated with vertical dotted lines.

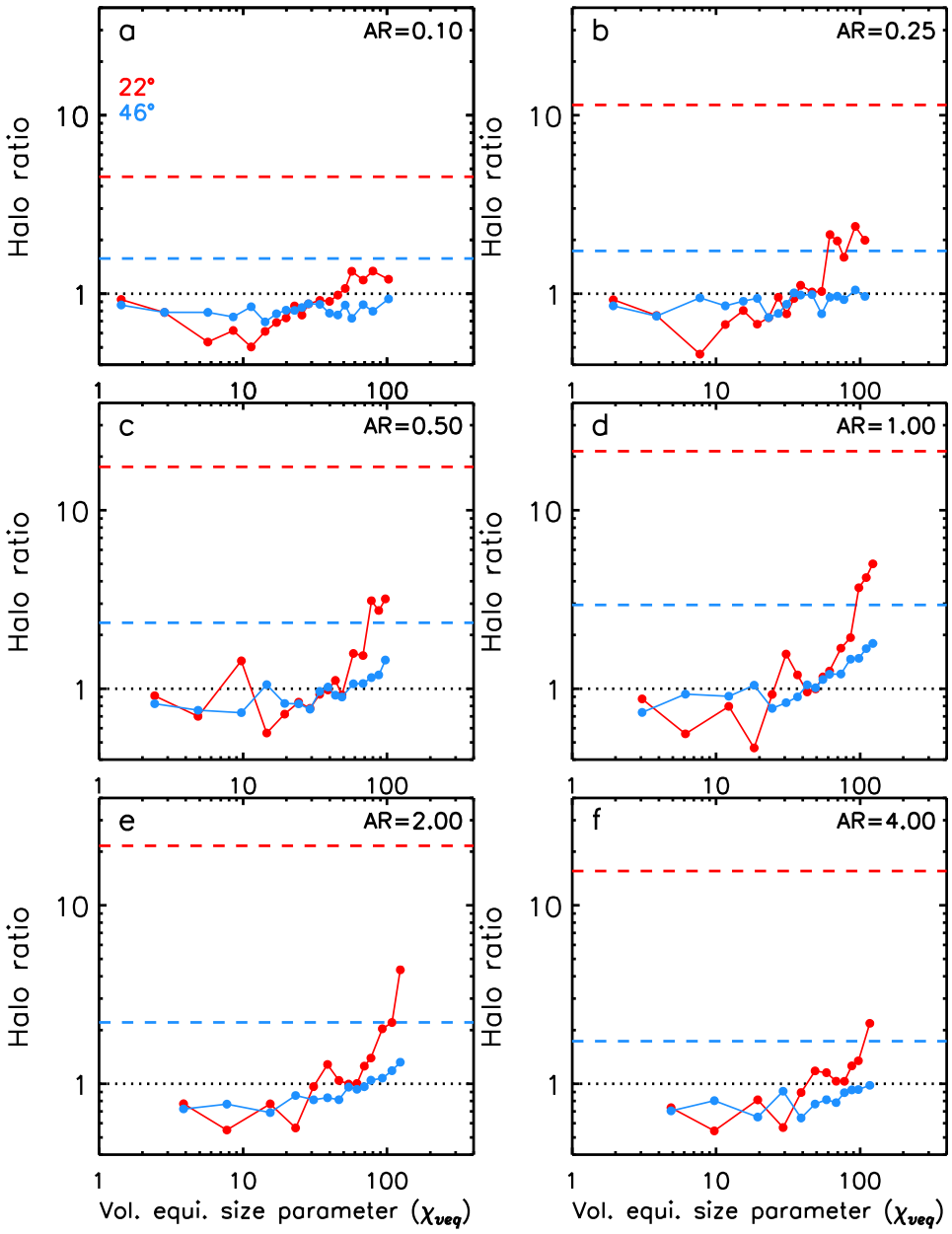

Figure 11: Calculated 22_ (red) and 46_ (blue) halo ratios of hexagonal crystals with (a) AR= 0.1, (b) AR= 0.25, (c) AR= 0.5, (d) AR= 1.0, (e) AR= 2.0, and (f) AR= 4.0 as a function of volume-equivalent-sphere size parameter. The DDA simulations are shown with the circles and solid lines, while the geometric optics method simulations are shown with dashed color lines. The halo ratio of 1.0 is shown with black dotted line in each panel..